

Chapter 6

The All-Sky Survey

6.1 Introduction

When astronomers first look at the sky with a new tool, they first survey the whole sky for point sources. Muon astronomy should be no exception. Rather than biasing the search for muons of astrophysical origin toward any particular source, the whole sky must be examined methodically, to see if anything stands out. Should an individual source such as the quasar 3C273 exist at a detectable level, it will be seen in an all-sky survey. However, no *a priori* choice is made that any individual source should or should not exist if the whole sky is treated equally. The detection of a source is defined to be a DC excess of muons in a bin on the sky that is inconsistent with a gaussian fluctuation in the background to a level specified *a priori*. In the event that the data coming from any particular part of the sky is more consistent with background than the hypothesis of a source, then an upper limit to the muon flux from an astrophysical point source in that section of sky can be established.

6.2 MACRO's Angular Resolution

To perform the most sensitive search for muon point sources, the angular resolution of MACRO needs to be determined. For an all-sky survey, the sky needs to be divided into bins of a size that would maximize the signal-to-noise ratio in any

given angular bin on the sky, where the noise is a combination of the statistical noise in the signal and the background of cosmic ray-induced muons. If the bin is too large, too many background muons are included, overwhelming the signal coming from an astrophysical source. If the bin is too small, the statistical fluctuations in the few muons falling into the bin far too often mimic an excess.

The angular resolution of MACRO enters into this binning question as follows. If MACRO is incapable of pointing muons back onto the sky with a great deal of accuracy, then the signal muons will appear to be spread out in a larger area of space on the sky. This requires a larger bin to capture the signal muons; unfortunately it also allows many background muons to enter the bin. However, if MACRO can resolve the muons' angles well, then any signal will be concentrated in a smaller area, thereby allowing a smaller bin size to keep the background low. To answer the question of bin size, it is necessary to know where on this scale MACRO's angular resolution lies.

6.2.1 The Tracking Resolution of MACRO

The intrinsic angular resolution of MACRO is easy to determine. The error in the angle of any given muon track is due to the granularity of the streamer tube hits from which the track is constructed. A streamer tube hit can be resolved in space with an accuracy of 4.5 cm in the wire view and 8.96 cm in the strip view¹. For muons traversing the lower part of MACRO, the lever arm between the top and bottom hits in the track is on the order of the height of MACRO, or 4.8 m. This results in a purely geometrical error of $\sin^{-1}(2 \times 4.5)/4800 = 0.11^\circ$ in the wire view, and

$\sin^{-1}(2 \times 8.96)/4800 = 0.21^\circ$ in the strip view. The binning of the moon data into 0.2° bins in Chapter 4 was driven by these numbers.

6.2.2 MACRO's Actual Point Spread Function

However, as discussed in Chapter 4, the dominant error in reconstructing the arrival direction of a muon with MACRO is the multiple Coulomb scattering experienced by the muon in the rock overburden above MACRO. To get a better estimate of MACRO's actual angular resolution, the relative scatter of the components of double muon pairs was used to generate a Point Spread Function (PSF) (Chapter 4).

6.2.3 Monte Carlo Studies to Optimize the Binning

The moon is an extended object rather than a point source. Thus the observed moon shadow cannot simply be inverted from a sink to a source, nor studied to determine the optimum bin size to look for point sources of muons. To remedy this, a simple Monte Carlo was written which created Poissonian fluctuations about a mean background in a grid of bins of size 0.2° on a side. Poissonian fluctuations were used due to the low number of counts (~ 30) seen by MACRO in a typical 0.2° bin. This number is on the boundary between Poissonian and Gaussian statistics, so Poissonian statistics were used to be conservative. A number of simulated muons were scattered onto this grid using the PSF derived from double muons. The resulting surplus of muons over background was binned into a histogram of surplus versus radius from the center of the PSF, in the same style figure shown for the deficit near the moon in Chapter 4. Figure 1 shows an example of this simulation.

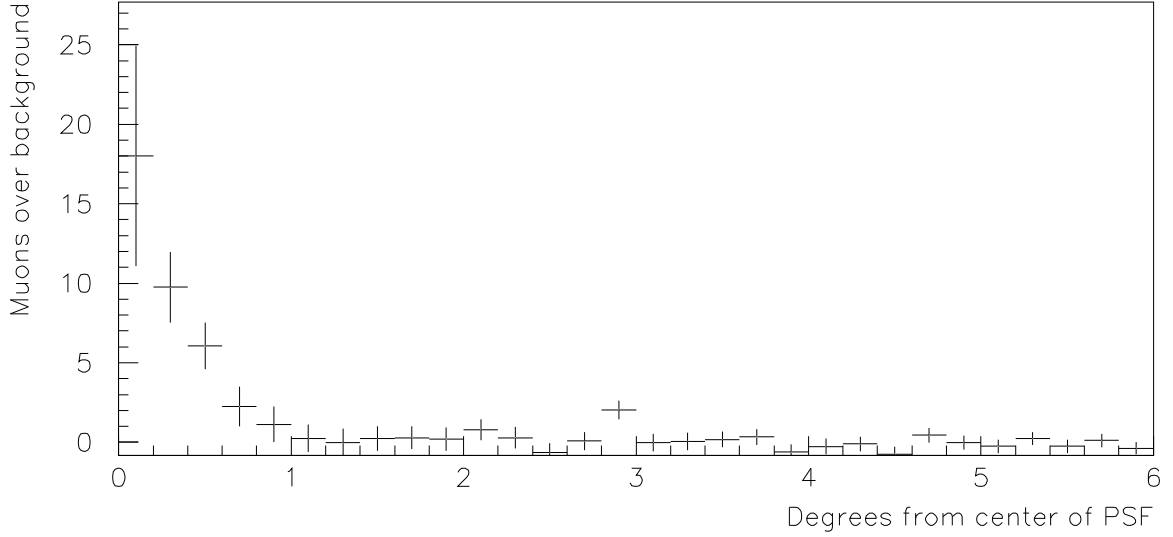


Figure 1: A simulated source, excess over background vs. radius. This simulation had a mean N_{back} of 30, and 425 simulated muons were scattered using MACRO's PSF.

The goal of this simulation is to determine at what radius the signal to noise ratio of the data included inside that radius is maximized. The value maximized is the excess number of muons over background in terms of the Gaussian deviation

$$D_{\sigma} = \frac{(N_{obs} - N_{back})}{\sqrt{N_{back}}}, \quad (1)$$

where N_{obs} is the number of muons observed, and N_{back} is the number of muons expected. Both N 's are integrated from the center of the PSF to the radius in question. Gaussian statistics are valid for larger values of the integrated counts.

There are two variables for consideration in this process. The first is the value of the mean background. To match the sky conditions in the real data sample, a mean

background of 30 events per bin was chosen. This number is comparable to the background per bin seen in the moon survey, which is a fair average of the large region of the sky through which the moon passes in its orbit.

The next variable is the strength of the simulated source, or the number of muons which are scattered onto the background using the PSF. Since the goal of this process is to choose a bin size maximizing MACRO's sensitivity to point sources, the strength of the simulated source should be that which produces the minimum statistically significant excess. As discussed in Section 6.5.2, an individual bin needs an excess of more than 5.5σ to be significant in this search. Thus, the number of muons in the simulated signal was set to produce an excess of greater than 5.5σ .

A number of such Monte Carlo simulations were made. During these simulations, the simulated source strength was varied, and the deviation of excess muons inside various radii was computed using Equation 1. This process demonstrated the signal to noise ratio was maximized for radii near $\frac{1}{2}^\circ$ for a 5.5σ excess inside this radius. This corresponds to a bin in an all-sky survey of 1° on a side. Note the PSF as derived from double muons is the number of muons in a pair falling within a given space angle of each other. For these $\frac{1}{2}^\circ$ radius bins, 41.3% of the muons fall inside.

6.3 The Data Binning

The data used in the all-sky survey are the same muons used in the search for the moon's shadow in Chapter 4 and discussed at length in Chapter 3. The muon

arrival directions are binned into a grid in right ascension (α) and $\sin(\text{declination})$ ($\sin \delta$). The use of the sine function allows a square grid to contain bins of equal solid angle when translated from the spherical coordinate system of (α, δ) . The bins are spaced 1° apart in α , and $1/75$ in $\sin \delta$, providing a solid angle of slightly less than one square degree. This choice of bin size was motivated by the $1/2^\circ$ radius signal to noise optimization discussed in Section 6.2.3.

However, the optimization of bin size for MACRO's PSF is only valid if the point source in question lies in the center of the bin. If the source is near a bin's edge and spreads its signal out between adjacent bins, then sensitivity is lost. Thus, three additional surveys were performed with different binning. The size of the grids remained the same, but the bin edges were offset by one-half a bin width to allow a source falling near an edge in one survey to be near a bin center in one of the other surveys. The second survey shifted the grid one-half bin in α ; survey number three shifted the grid down one-half bin in $\sin \delta$; survey four contained both shifts.

The two surveys incorporating a shift in declination needed additional bins near the celestial north pole, because the top edge of what had been the topmost bin was shifted downwards, leaving uncovered area near the north pole. This area was binned into one circular polar bin of approximately equal solid angle to the square bins in the main grid, and a ring of 177 more square bins of about the same solid angle covering the area between the cap and the main grid.

6.4 Background Calculations

In order to determine the expected level of isotropic muons in each of the bins in the four surveys, the Monte Carlo technique described in Chapter 3 was used to generate simulated data sets. These simulated data sets contain no point sources of excess muons. They only contain the background of isotropic cosmic ray induced muons providing the bulk of MACRO's signal. The muons generated by these Monte Carlos were binned in the same manner as the real data in the four survey grids. In order to get an expected background for each bin free from statistical fluctuations, 717 such datasets were averaged. The results of this process were values of the expected background for each bin in the four surveys.

6.5 Gaussian Deviations in the Muon Sky

For each bin in the four surveys containing above 5% of the average number of muons present in circumpolar bins (70.6 muons), the Gaussian deviation of Equation 1 was calculated, taking N_{obs} from the real data grids, and N_{back} from those calculated by the Monte Carlos. This 5% cutoff was chosen because the exposure of bins at low $\sin \delta$ is quite small. For bins below this cutoff, statistical fluctuations dominate.

6.5.1 The Observed Deviations

If the observed muons are distributed according to Gaussian statistics, the distribution of values of D_σ calculated from the real data will fall along a Gaussian curve of mean zero and width one. If there is an astrophysical source of muons, the bin in which that source is centered will have a large positive D_σ that is inconsistent

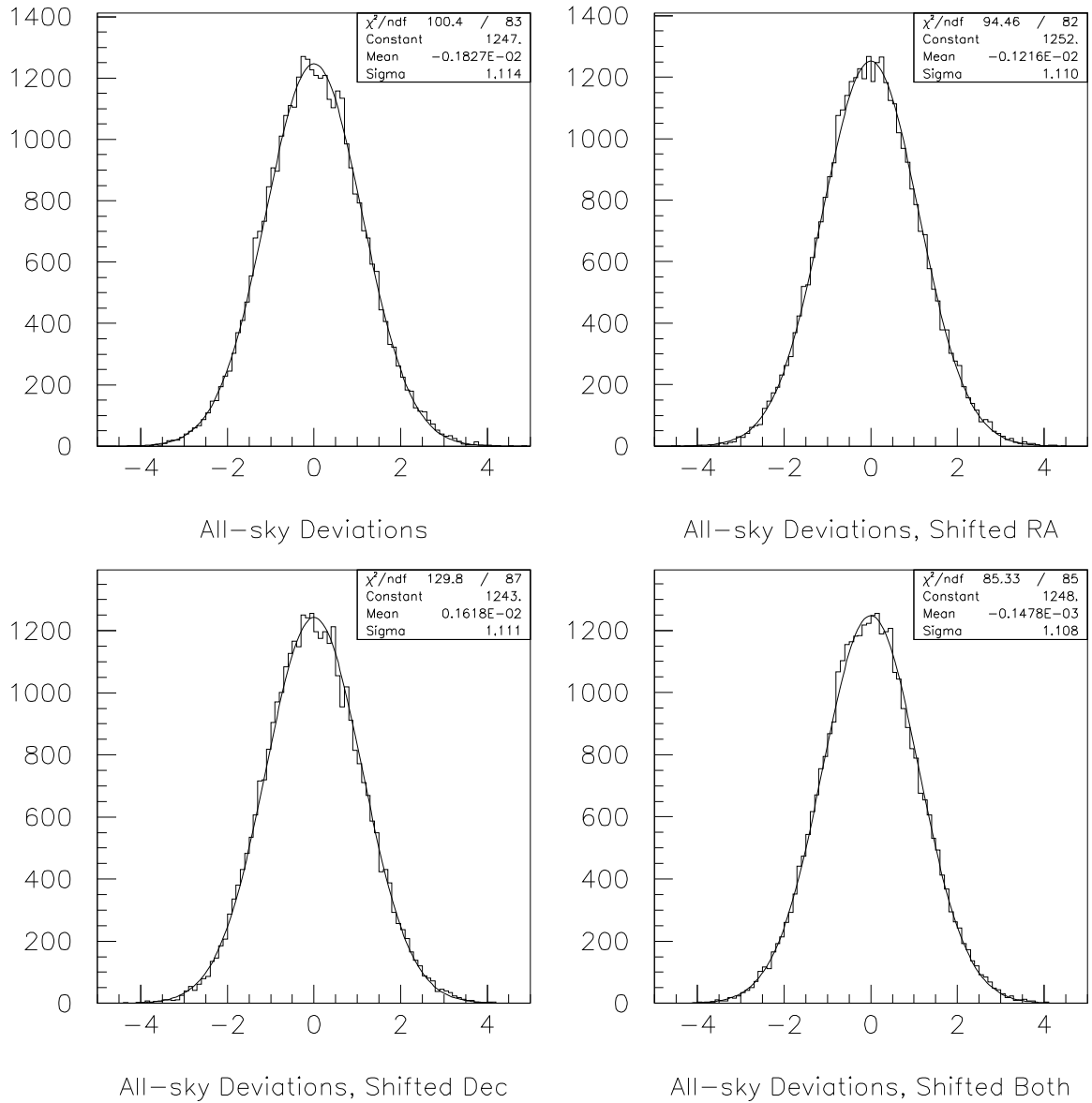


Figure 2: Distributions of D_σ for the four all-sky surveys, and their best fit Gaussian curves.

with belonging to the tail of the Gaussian curve. The distributions of D_σ for the four surveys are shown in Figure 2, with the best fit Gaussian curves superimposed.

Survey	# of bins	Mean	Width	X ² /DoF
(1) Unshifted	34,920	-1.83e-03	1.11	1.21
(2) Shifted in α	34,920	-1.22e-03	1.11	1.15
(3) Shifted in $\sin \delta$	34,738	1.62e-03	1.11	1.49
(4) Shifted in both	34,738	-1.48e-04	1.11	1.00

Table 1: Gaussian fit parameters for the D_σ distributions in Figure 2.

The best fit Gaussian curves to the D_σ distributions from the four surveys are listed in Table 1. These curves are all of mean near zero and width near one as expected for a Gaussianly distributed real data sample. The tails of the distribution are of interest to this analysis, as they are where a real source would be hiding. A list of all deviations of absolute magnitude $D_\sigma \geq 4.5\sigma$ is given in Table 2.

Survey, Position (α h, δ °)	N_{obs}	N_{back}	D_σ	Probability (%)
1,(19.9,32.2)	1124	980.43	4.59	63.1
1,(9.27,49.5)	1203	1044.92	4.89	18.4
2,(14.9,-8.43)	262	346.56	-4.54	74.6
3,(1.20,-14.3)	190	136.17	4.61	56.2
3,(5.73,45.5)	837	983.87	-4.68	42.7
4,(14.9,-8.05)	276	363.39	-4.58	63.0
4,(0.63,0.38)	834	701.79	4.99	12.0

Table 2: List of large D_σ . Position is the lower left bin corner.

There are a significant number of large negative deviations in this list. Such deviations are certainly due to statistical fluctuations in the data. The presence of

large negative fluctuations implies there should be a similar number of large positive fluctuations arising from the same statistics. The “Probability” entry in Table 2 is the chance that a statistical fluctuation of that magnitude or larger will occur for the number of bins in that survey listed in Table 1 and given a Gaussian distribution as fit in Figure 2. All these fluctuations are consistent with Gaussian fluctuations in the standard cosmic ray sky, and do not correspond with the positions of any known high energy astrophysical sources².

Something else to consider is the fact that the same data has been examined four times. This magnifies the chances of finding a fluctuation, simply due to the process of examining the data four different ways. Since the four surveys are not independent (as witnessed by the survey #2 fluctuation and the first of the survey #4 fluctuations), the probability of finding a fluctuation is not multiplied by a factor of four. The true factor lies somewhere between one and four, but the statistics of the exact factor have not been pinned down.

6.5.2 Source Criterion

How large a deviation would be considered a background fluctuation? A common level of acceptance for something new is either a “Three Sigma” or a “Five Sigma” detection. Using standard Gaussian probabilities, this corresponds to 0.27% or a 0.000057% chance of a background fluctuation mimicking a signal³. Given the number of bins in any one of the four surveys, this corresponds to a $D_\sigma \geq 5.5\sigma$ for a “Three Sigma” detection, or $D_\sigma \geq 6.4\sigma$ for a “Five Sigma” detection. Thus, if a bin in one of the four surveys presented above has $D_\sigma \geq 5.5\sigma$, the hypothesis that the bin

contains some source of muons other than an isotropic background would have to be taken seriously.

6.6 Flux Limits

To what flux level is MACRO sensitive if there were a real astrophysical muon source? Indeed, there must be sources at some level due to UHE gamma rays producing some muons (see Chapter 1). Should MACRO detect these gamma rays? The upper limit of a flux to which this analysis would have been sensitive has been calculated at the 95% confidence limit (CL). The number of muons per square centimeter per second which MACRO would have just barely detected had such a signal been present has been calculated for each bin on the sky. This number is

$$J_{\mu}^{stdy}(95\%) \leq \frac{n_{\mu}(95\%)}{0.41 \bar{\epsilon} A_{eff} f t_{expos}} \text{ cm}^{-2} \text{ s}^{-1}, \quad (2)$$

where $n_{\mu}(95\%)$ is the 95% CL for the just barely undetected number of muons in the bin, ϵ is the average efficiency, A_{eff} is the average effective area, f is the fractional exposure time, and t_{expos} is the total exposure time. All of these numbers except for t_{expos} vary from bin to bin, and t_{expos} (given in Chapter 3) is 44,377.87 hours. The constant factor of 0.41 is the fraction of the muons which scatter outside the $\frac{1}{2}^{\circ}$ bin, as discussed in Section 6.2.2.

Helene⁴ has shown that for data consistent with a Gaussian distribution of statistical fluctuations, $n_{\mu}(95\%)$ can be found from

$$\frac{2}{\sqrt{\pi}} \int_{n_{\mu}(95\%)}^{\infty} \frac{e^{-(n_{\mu}-\bar{n}_{\mu})^2/2\sigma^2}}{\sqrt{2}\sigma} dn_{\mu} = 0.05 , \quad (3)$$

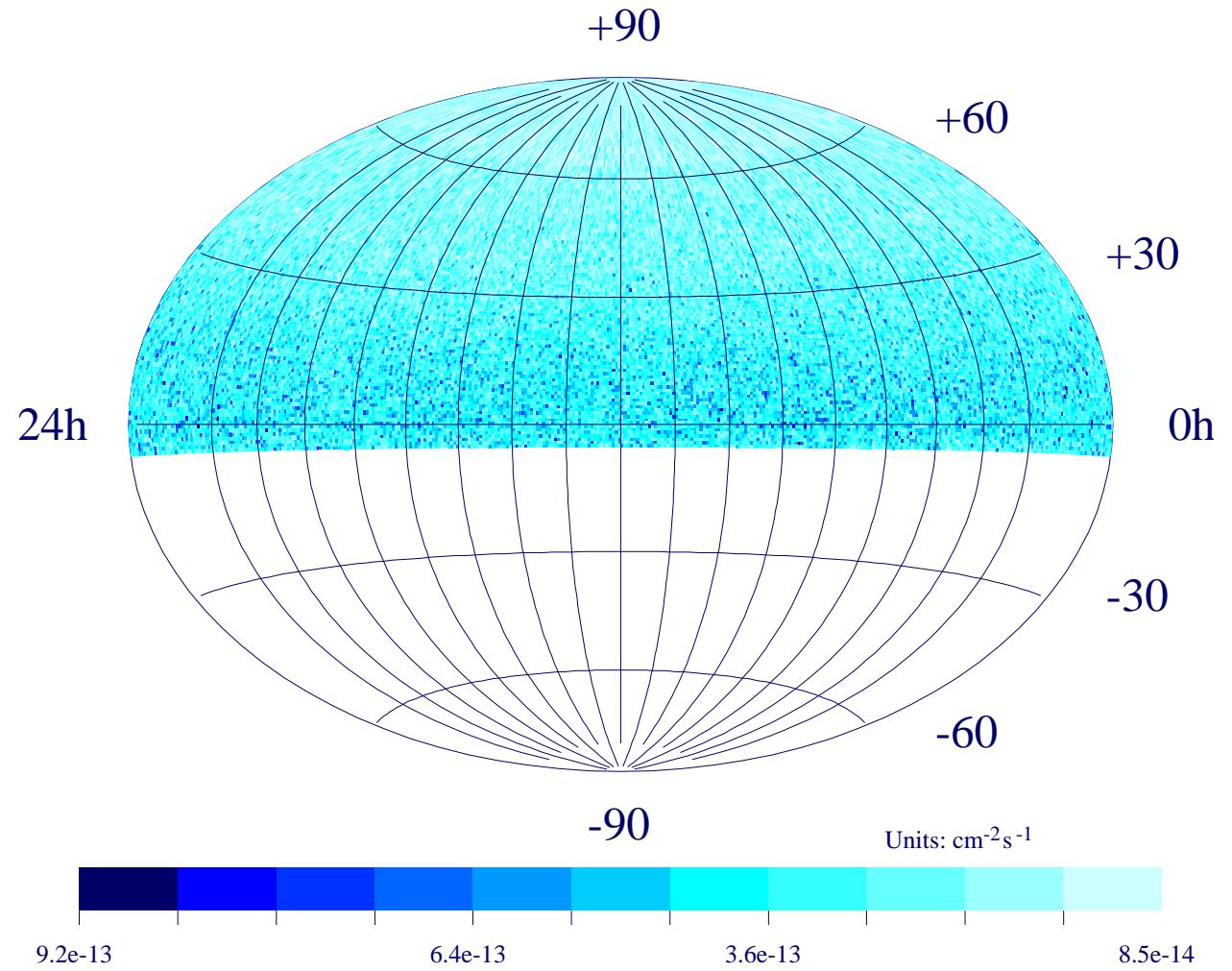
where $\bar{n}_{\mu} = n_{obs}-n_{back}$ and $\sigma^2 = n_{obs}-n_{back}$.

The term ϵA_{eff} is calculated for each bin by averaging the efficiency times effective area seen by each muon that falls in the bin. For each muon, this geometrical efficiency is determined from a table of such values computed by exhaustive, GEANT-based Monte Carlo calculations of MACRO's efficiency as a function of the angle of incidence of a muon upon MACRO⁵. The final value needed is f , the fractional exposure for each bin. This is calculated by incrementing a counter for each bin on the sky that meets the 72° zenith angle cut at the time of each observed muon, then dividing this counter by the total number of muons observed. The values of $J_{\mu}^{stdy}(95\%)$ for each bin on the sky have been calculated in this manner and are displayed in Figure 3. Limits such as these have been compared to source models and luminosities by Miller⁶, severely constraining many models of the production of muon parents in astrophysical sources.

ALL-SKY SURVEY

95% Confidence Limits on Muon Flux

Figure 3: All-sky map of DC muon flux limits, in units of $\mu \text{ cm}^{-2} \text{ s}^{-1}$.



6.7 Conclusions

All the bins in all four all-sky surveys are consistent with the hypothesis that no point sources of muons are present in this data. All deviations from the expected background are consistent with Gaussian fluctuations in the expected background of isotropically distributed primary cosmic rays.

The smallest upper limit in this survey was

$$J_{\mu}^{stdy}(E_{\mu} \geq 1.2 \text{ TeV}) = 8.5 \times 10^{-14},$$

which is still well above the muon flux due to UHE gamma rays of

$$J_{\mu\gamma}(E_{\mu} \geq 3 \text{ TeV}) \approx 10^{-15} \text{ cm}^{-2} \text{ s}^{-1}$$

as calculated by Berezhinsky⁷ for Cygnus X-3. Therefore, the lack of any significant excesses is consistent with the standard model.

References

1. Ahlen, S. *et al.*, The MACRO Collaboration, 1993, “The First Supermodule of the MACRO Detector at Gran Sasso”, *Nucl. Instr. and Methods in Physics Research A* **322**, 101.
2. Seward, F.D., and Martenis, P., 1986, **Catalog of Einstein (HEAO-2) Observations**, 5th ed., Harvard-Smithsonian Center for Astrophysics, Cambridge MA.
3. Bevington, P.R., and Robinson, D.K., 1992, **Data Reduction and Error Analysis for the Physical Sciences**, 2nd ed., McGraw-Hill Inc., New York.
4. Helene, O., 1983, “Upper Limit of Peak Area”, *Nucl. Instr. and Meth.* **212**, 319.
5. Ambrosio, M. *et al.*, The MACRO Collaboration, 1995, “Vertical Muon Intensity Measured with MACRO at the Gran Sasso Laboratory”, *Phys. Rev. D* **52**, 3793.
6. Miller, J.L., 1994, **A Search for Cosmic Ray Point Sources of Muons and for Seasonal Variations in Underground Muon Flux with the MACRO Detector**, Indiana University, unpublished PhD dissertation.
7. Berezinsky, V.S., Cini-Castagnoli, G., Kudrayavtsev, V.A., Ryazhskaya, O.G., Zatsepin, G.T., 1988, High Energy Gamma-Astronomy with Large Underground Detectors”, *Astronomy and Astrophysics* **189**, 306.